J Solid State Electrochem (2010) 14:1533–1539
DOI 10.1007/s10008-009-0984-1

ORIGINAL PAPER

Asymmetric supercapacitors based on stabilized α-Ni(OH)$_2$ and activated carbon

Jun-Wei Lang · Ling-Bin Kong · Min Liu · Yong-Chun Luo · Long Kang

Received: 23 March 2009 / Revised: 19 November 2009 / Accepted: 20 November 2009 / Published online: 15 December 2009

Abstract In this work, stabilized Al-substituted α-Ni(OH)$_2$ materials were successfully synthesized by a chemical coprecipitation method. The experimental results showed that the 7.5% Al-substituted α-Ni(OH)$_2$ materials exhibited high specific capacitance (2.08×10^3 F/g) and excellent rate capability due to the high stability of Al-substituted α-Ni(OH)$_2$ structures in alkaline media, suggesting its potential application in electrode material for supercapacitors. To enhance energy density, an asymmetric type pseudo/electric double-layer capacitor was considered where α-Ni(OH)$_2$ materials and activated carbon act as the positive and negative electrodes, respectively. Values for the maximum specific capacitance of 127 F/g and specific energy of 42 W·h/kg were demonstrated for a cell voltage between 0.4 and 1.6 V. By using the α-Ni(OH)$_2$ electrode, the asymmetric supercapacitor exhibited high energy density and stable power characteristics. The hybrid supercapacitor also exhibited a good electrochemical stability with 82% of the initial capacitance over consecutive 1,000 cycle numbers.

Keywords Asymmetric supercapacitors · Alpha-nickel hydroxide · Specific capacitance · Specific energy

J.-W. Lang · L.-B. Kong (✉) · M. Liu
State Key Laboratory of Gansu Advanced Non-ferrous Metal Materials, Lanzhou University of Technology, Lanzhou 730050, People's Republic of China
e-mail: konglb@lut.cn

Y.-C. Luo · L. Kang
Key Laboratory of Non-ferrous Metal Alloys and Processing of Ministry of Education, Lanzhou University of Technology, Lanzhou 730050, People's Republic of China

Introduction

Supercapacitors are currently investigated in various academic and industrial laboratories because they can provide a higher energy density than dielectric capacitors and a higher power density than batteries [1–3]. However, compared to rechargeable battery systems, supercapacitors still present a very important drawback (e.g., the amount of energy density is relatively low) and preclude the extensive industrial utilization in energy storage [4–6]. Therefore, in order to satisfy the industrial demand, the performance of supercapacitors must be improved. The development of new materials and new concepts has enabled important breakthroughs during the last years.

Recently, asymmetric or hybrid supercapacitor, regarded as the trend in electrochemical capacitors, has been reported. Asymmetric supercapacitor can be fabricated with one electrode being of a double-layer carbon material and the other electrode being of a pseudo-capacitance material. It is possible to reach the high working voltage and high energy density by choosing a proper electrode material, contributed to a significant increase in the overall energy density of the supercapacitor devices [7–9].

The electrodes of supercapacitors make use of three main classes of materials: Carbon [10, 11], metal oxide [12, 13], and electronically conducting polymer [14, 15]. Among these electrode materials, activated carbon (AC) with various modifications is the electrode material used most frequently for electrode of supercapacitors. Charge storage on carbon electrodes is predominantly capacitive in the electrochemical double layer. Carbon-based supercapacitors come close to what one would call an electrochemical double-layer capacitor (EDLC) [16]. Transition metal oxides such as ruthenium oxide [17, 18], manganese oxide [1, 19], cobalt oxide [20, 21], and nickel oxide [22, 23] are qualified to be

supercapacitor materials, because the capacitance of metal oxide electrode is mainly the result of the pseudo-capacitance, which originated from the electrical charge transport in redox reaction. However, although the capacitive performance of ruthenium oxide is excellent, it is too expensive for commercialization. Most of the attention is, therefore, focused on alternative electrode materials that are inexpensive and exhibit capacitive behavior similar to that of ruthenium oxide.

Nickel hydroxide materials have received increasing attention in recent years on account of their applications in alkaline secondary batteries, fuel cells, supercapacitors, electrolyzers, electrosynthetic cells, and electrochromic devices [24, 25]. The nickel hydroxide crystallizes in two polymorphic modifications known as α and β, a higher theoretical capacity for the nickel-positive electrode comprising α-$Ni(OH)_2$ is envisaged in relation to a β-$Ni(OH)_2$ electrode. However, α-$Ni(OH)_2$ happens to be unstable in alkaline medium and transforms to β-$Ni(OH)_2$ [26]. Previous studies show that the maximum specific capacitance of 3125 F/g for α-$Ni(OH)_2$, which is the highest reported for supercapacitor, was obtained by the electrodeposition method [27]. But the long-term electrochemical stability is relatively poor, it exhibited a loss of 48% in capacitance of α-$Ni(OH)_2$ electrode during the only 300 cycles. Therefore, a lot of research work have been done to prepare a stable α-$Ni(OH)_2$ material with high capacitance. In order to prepare a stable α-$Ni(OH)_2$, many studies have been carried out through partial substitution of nickel ion in the nickel hydroxide lattice by other metal ions such as Al, Co, Fe, Mn, and Zn. Among these metal elements, Al is the most attractive because Al-substituted α-$Ni(OH)_2$ has relatively better electrochemical performance [26, 28].

In our previous work [29, 30], loose-packed α-$Ni(OH)_2$ and NiO materials with two morphologies (amorphous particles and nanoflake phase) were synthesized by a facile precipitation method, the maximum specific capacitances of 2,055 and 942 F/g could be achieved in a half-cell setup configuration for the $Ni(OH)_2$ and NiO electrodes, respectively, suggesting their potential application in the electrode materials for supercapacitors. However, the long-term electrochemical stability of the α-$Ni(OH)_2$ material was very poor, it exhibited a loss of 70% in capacitance during the 1,500 cycles, the capacitance fading may originate from the slow transformation of α-$Ni(OH)_2$ to β-$Ni(OH)_2$. In this work, we reported on the preparation and electrochemical properties of Al-substituted α-$Ni(OH)_2$ materials, which were synthesized by a coprecipitation method. The results showed that the 7.5% Al-substituted α-$Ni(OH)_2$ materials exhibited high specific capacitance (2.08×10^3 F/g) and excellent rate capability due to the high stability of Al-substituted α-$Ni(OH)_2$ structures in alkaline media, which shows better rate capability and great potential as the electrode materials for supercapacitors. Unfortunately, the Al-substituted α-$Ni(OH)_2$ material has a narrow operation potential (the real galvanostatic discharge window is about 0.4 V), and it is thereby limited to practical applications because of energy density. Therefore, we first introduced this Al-substituted α-$Ni(OH)_2$ materials as a positive electrode to fabricate an asymmetric supercapacitor in combination with activated carbon as the negative electrode in 2 M KOH electrolyte solution. The primary electrochemical characterization was investigated by cyclic voltammetry (CV) and galvanostatic charge/discharge test. The effect of the microstructure on its electrochemical performance of the prepared material has also been systematically investigated.

Experimental

Materials preparation

All of the chemicals were of analytical grade and were used without further purification. Al-substituted α-$Ni(OH)_2$ materials were prepared by a coprecipitation method. Firstly, mixed two kinds of metal salts solution (1.5 M total concentration) containing $NiCl_2{\cdot}6H_2O$ and $Al_2(SO_4)_3$ in a glass beaker using a magnetic stir bar, the molar ratios of the $NiCl_2{\cdot}6H_2O/Al_2(SO_4)_3$ were 1:0.031; 1:0.042; 1:0.053; 1:0.067; and 1:0.083. The mixed metal salt solution was slowly adjusted to pH 9 by the dropwise addition of 5 wt.% NH_4OH at a temperature of ~10 °C, the NH_4OH solution was added dropwise with a constant time interval of 5 s. The resulting suspension was stirred at this temperature for an additional 3 h. Then the solid was filtered and washed with a copious amount of distilled water, and dried at 100 °C in air for 6 h. Commercial AC (The ShaoWu XinSen Carbon Company, China, with a specific surface area of 2,000 m^2/g and a diameter of 5–10 μm) was used as the negative electrode material without further treatment.

Structure characterization

To test for stability, 0.5 g of each sample was suspended in 20 ml of 6 M KOH for 15 days. The samples were removed after each stage, filtered, washed to neutral, and dried to constant weight at 100 °C. All the samples, after aging were characterized by powder X-ray diffraction (XRD) measurements (Bruker, D8 Advance, Germany). The elemental compositions in the as-prepared samples were determined by Inductively Coupled Plasma spectroscopy (TJA, IRIS Advantage ER/S, USA).

Preparation of the electrodes

The working electrodes were prepared according to the method reported in Ref. [31]. $Ni(OH)_2$ powder (80 wt.%)

was mixed with 7.5 wt.% of acetylene black (>99.9%) and 7.5 wt.% of conducting graphite in an agate mortar until a homogeneous black powder was obtained. To this mixture, 5 wt.% of poly (tetrafluoroethylene) was added with a few drops of ethanol. After briefly allowing the solvent to evaporate, the resulting paste was pressed at 10 MPa to a nickel gauze with a nickel wire for an electric connection. The electrode assembly was dried for 16 h at 80 °C in air. The AC electrodes were prepared by the same method as the negative electrode described above.

Electrochemical test of the single electrode and asymmetric supercapacitor

The electrochemical measurements of single $Ni(OH)_2$ and AC electrodes were carried out using an electrochemical working station (CHI660C, Shanghai, China) in a three-electrode cell at room temperature. A platinum gauze electrode and a saturated calomel electrode (SCE) served as the counter electrode and the reference electrode, respectively. Each electrode contained about 8 mg of electroactive material and had a geometric surface area of about 1 cm^2.

The $Ni(OH)_2$ cathode and AC anode were pressed together and separated by a porous nonwoven cloth separator. The mass ratio of active materials (anode/cathode) was 37.3:8 mg. Each electrode had a geometric surface area of about 1 cm^2. The electrochemical measurements of the asymmetric supercapacitor were also carried out using the electrochemical working station in a two-electrode cell at room temperature.

The specific capacitance of the asymmetric capacitor can be evaluated from the charge/discharge test together with the following equation:

$$C = I/[(dE/dt) \times m] \approx I/[(\Delta E/\Delta t) \times m] \quad (F/g) \qquad (1)$$

where C is the specific capacitance; I is the constant discharging current; Δt is the time period for the potential change ΔE; and m is the mass of the corresponding electrode materials measured.

The charge on the electrode can be evaluated from the charge/discharge test together with the following equation:

$$C' = I\,\Delta t/m \quad (C/g) \qquad (2)$$

where I is the constant discharging current; Δt is the time period for the potential change; and m is the mass of the corresponding electrode materials measured.

The real power density P_{real} is determined from the constant current charge/discharge cycles as follows [32]:

$$P_{real} = \Delta E I/m \quad (W/kg) \qquad (3)$$

where $\Delta E = (E_{max} + E_{min})/2$ with E_{max} is the potential at the end of the charge and E_{min} at the end of the discharge, I is the applied current (A), and m is the weight of the active material in the electrode (kg).

The specific energy E_{real} is defined as

$$E = C\left(E_{max}^2 - E_{min}^2\right)/2 \quad (W \cdot h/kg) \qquad (4)$$

where C is the system capacitance for a cell and E_{max} is the potential at the end of charge and E_{min} at the end of discharge.

Results and discussion

Characterization of materials

Table 1 shows the atomic percentages (at.%) of the elements Al and Ni in Al-substituted $Ni(OH)_2$ samples, obtained by ICP spectroscopy. Using this information, several electrodes containing various Al levels were prepared for testing, and their results will be systematically discussed hereafter.

The XRD patterns of the aged samples are shown in Fig. 1. The 7.5% and 9.16% Al-substituted $Ni(OH)_2$ samples do not show any structural changes and stabilize the α-$Ni(OH)_2$ structure after ageing in 20 ml of 6 M KOH for 15 days at room temperature, the general features of all the diffraction patterns obtained for all the samples were similar to the standard XRD pattern of α-$Ni(OH)_2 \cdot 0.75H_2O$ (JCPDS 22-444). In contrast, the sample without any Al has completely transformed to β-phase. In the pattern of 4.72% Al-substituted α-$Ni(OH)_2$ sample, no peaks of β-phase appear, but the peaks of α-phase have also become wider and weaker after ageing for 15 days at the room temperature. The result shows that the addition of Al over 7.5% leads to higher crystallinity and increases the structure stability in alkaline medium [26, 33].

The electrochemical characterizations of the Al-substituted α-$Ni(OH)_2$ materials and AC

To evaluate the electrochemical properties of the as-prepared Al-substituted α-$Ni(OH)_2$ materials, we directly use these materials to fabricate electrodes for supercapacitors. Chronopotentiometry measurement has been used to evaluate the electrochemical properties and quantify the specific capacitance of the as-prepared $Ni(OH)_2$ electrode. Figure 2a shows the discharging curves of the electrode using α-$Ni(OH)_2$ containing various Al contents in the potential range of 0–0.4 V in 2 M KOH at the current rates of 5 mA. The shape of the discharge curves does not show the characteristic of the pure double-layer capacitor but mainly pseudo-capacitance. It also can be seen that the discharge potential increase with increase in Al content. The specific capacitances of the α-$Ni(OH)_2$ with different Al contents electrodes at current densities of 5 mA/cm^2 were 2.24×10^3, 2.03×10^3, 2.05×10^3, 2.08×10^3, 1.92×10^3, and 1.85×10^3 F/g, corresponding to the different Al

Table 1 Composition of Al-substituted α-Ni(OH)$_2$

Ni/Al ratio in solution	Ni (atomic, %)	Al (atomic, %)	Denomination
1: 0.031	95.28	4.72	4.72% Al-substituted α-Ni(OH)$_2$
1: 0.042	92.74	7.26	7.26% Al-substituted α-Ni(OH)$_2$
1: 0.053	92.5	7.5	7.5% Al-substituted α-Ni(OH)$_2$
1: 0.067	91.16	8.84	8.84% Al-substituted α-Ni(OH)$_2$
1: 0.083	90.84	9.16	9.16% Al-substituted α-Ni(OH)$_2$

contents of 0%, 4.72%, 7.26%, 7.5%, 8.84%, and 9.16%, respectively. Figure 2b shows the effect of Al contents on the rate capability of the α-Ni(OH)$_2$ electrodes. The result shows that the capacity fading is suppressed at high current in Al-substituted materials. The specific capacitance of 7.5% Al-substituted α-Ni(OH)$_2$ electrode under the large current density of 100 mA/cm^2, was 71.5% of the initial capacitance can be reached, suggesting that Al-substituted α-Ni(OH)$_2$ can be used as high rate discharge electrode material. While the specific capacitance of pure Ni(OH)$_2$ electrode strongly decreased, and under the large current density of 100 mA/cm^2, only 8.5% of the initial capacitance can be reached. So the excellent rate capability of the Al-substituted α-Ni(OH)$_2$ samples makes it attractive particularly for a practical application.

To evaluate the electrochemical properties of the prepared 7.5% Al-substituted α-Ni(OH)$_2$ electrode and the commercial AC, we directly use these two materials to fabricate electrodes for supercapacitors. CV and chronopotentiometry measurements have been used to evaluate the electrochemical properties and quantify the specific capacitance of the 7.5% Al-substituted α-Ni(OH)$_2$ and AC electrodes. CV curves for AC and α-Ni(OH)$_2$ electrodes in 2 M KOH aqueous solution are shown in Fig. 3a. The AC electrode was performed within a potential window of −1.0 to 0 V (vs SCE) and α-Ni(OH)$_2$ was employed within a potential window of −0.2 to 0.7 V (vs SCE) at a scan rate of 5 mV/s. For the AC electrode, nearly rectangular CV curve is obtained, indicating a typical EDLC behavior because no peaks of oxidation and reduction are observed. It is suggested that the AC electrode can be used as a negative electrode at a potential window of −1 to 0 V (vs SCE) without the evolution of H_2 and O_2. The CV shapes

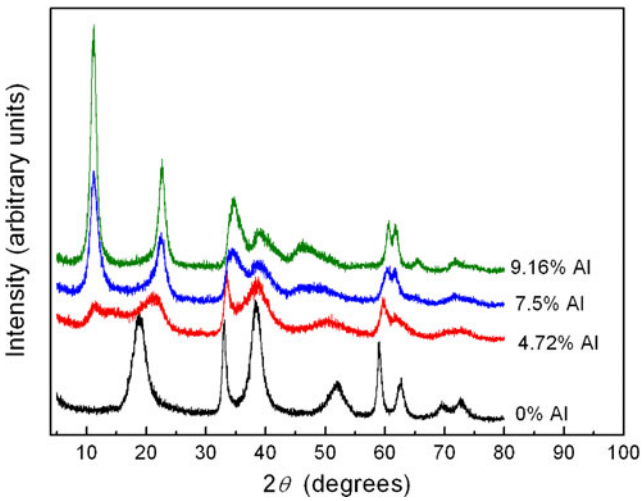

Fig. 1 XRD patterns of Al-substituted α-Ni(OH)$_2$ materials with different Al contents after aging in 6 M KOH at ambient temperature for 15 days

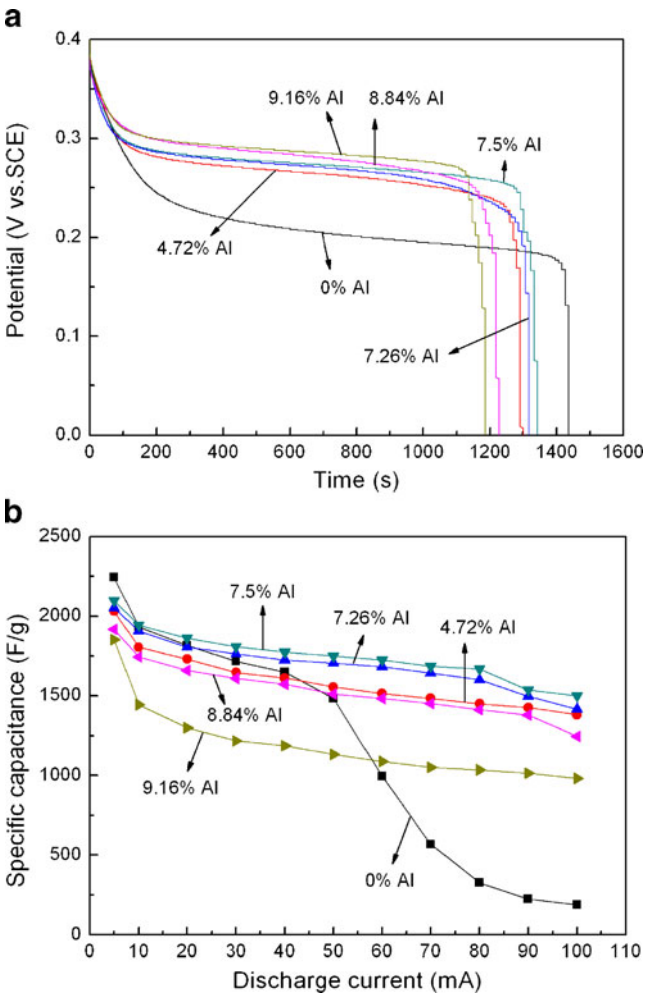

Fig. 2 **a** Discharging curves of the electrode using α-Ni(OH)$_2$ with various Al contents in the potential range of 0–0.4 V in 2 M KOH at a current density of 5 mA/cm^2; **b** The specific capacitance of Al-substituted α-Ni(OH)$_2$ materials with different Al contents as a function of discharge currents. The working electrodes have a geometric area of 1 cm^2 and contain 8 mg of Ni(OH)$_2$ (Vs. SCE)

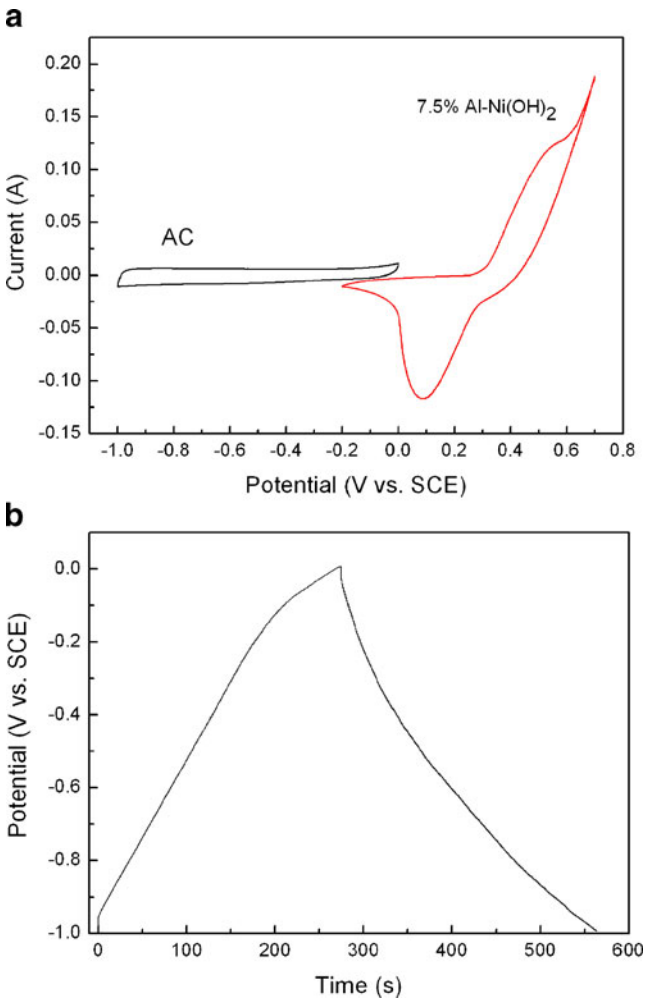

Fig. 3 **a** Cyclic voltammogram of AC and 7.5% Al-containing α-Ni$(OH)_2$ electrode at a scan rate of 5 mV/s in 2 M KOH solution; **b** Charge/discharge curves the AC electrode in the potential window of −1 to 0 V at a current density of 5 mA/cm^2 in 2 M KOH solution. Each electrode contained about 8 mg of electroactive material and had a geometric surface area of about 1 cm^2

of 7.5% Al-substituted α-Ni$(OH)_2$ electrode reveal that the capacitance characteristic is very different from that of the electric double-layer capacitance, two redox peaks are clearly observed. These indicate that the capacity mainly results from the pseudo-capacitance, which is based on a redox mechanism. The two strong redox reaction peaks are responsible for the pseudo-capacitance, the anodic peak is due to the oxidation of $Ni(OH)_2$ to NiOOH, and the cathodic peak is for the reverse process.

The linear charge/discharge curves are observed in Fig. 3b of the AC electrode within a potential window of −1 to 0 V at a current density of 5 mA/cm^2. The linear shape of the curve is attributed to the linear correlation of the absorbed charge on the interface with the applied potential. That means the specific capacitance is independent of the applied potential nature, distinctly accompanied with a nonfaradaic process on the interface. The charge on the AC electrode is 176 C/g in the potential window of −1 to 0 V, the charge on the 7.5% Al-substituted α-Ni$(OH)_2$ electrode and in the potential window of 0 to 0.4 V is 821 C/g, according to the Eq. 2. Therefore, the optimal mass ratio of the 7.5% Al-substituted α-Ni$(OH)_2$ electrode and the AC electrode is 176:821, and the loads of the cathode 7.5% Al-substituted α-Ni$(OH)_2$ electrode and the AC anode electrode materials are of 8 and 37.3 mg, respectively.

The electrochemical characterizations of the asymmetric capacitors

It is very important to polarize each electrode at the same potential before cycling the device; otherwise there is a risk of damaging the cell during the early cycles. The typical CV of the asymmetric capacitor at voltage scan rates of 2.5, 5, and 10 mV/s is depicted in Fig. 4a. The hybrid device was cycled between 0.4 and 1.6 V with a good reversibility in this potential window. At a fully oxidized state, 7.5% Al-substituted α-Ni$(OH)_2$ electrode gives about 0.6 V but the AC electrode gives about −1 V at a fully reduced state, whereas the discharge process proceeds until the potential of both electrodes is the same. Thus, the potential of the asymmetric unit cell can reach 1.6 V in the fully charged state. It should be noted that the CV curves can be approximately considered as rectangle shapes when the scan rate is 2.5 mV/s; when the scan rate increases to 5 mV/s, the curve begins to deform. Also, the current increases with scan rate, indicating rapid *I*–*V* response.

Galvanostatic constant current charge/discharge measurements at different current densities were applied to evaluate the electrochemical properties and to quantify the specific capacitance of the asymmetric supercapacitor in 2 M KOH electrolyte. Figure 4b shows the typical galvanostatic charge–discharge curves of the hybrid capacitor between 0.4 and 1.6 V at different current densities. As shown in Fig. 4b, during the charging and discharging steps, though an almost linear variation in the cell voltage is observed in the curves, perfect linear curves are not obtained compared with EDLC. This is due to a typical pseudo-capacitance behavior resulting from the electrochemical adsorption/absorption or redox reactions at interfaces between electrodes and electrolyte [32]. On account that the real galvanostatic discharge window of the 7.5% Al-substituted α-Ni$(OH)_2$ electrode is about 0.4 V, the result of the present work shows that it is possible to reach the high working voltage by choosing a proper electrode material. Furthermore, as the discharge current increases, the large voltage drop is produced and finally the capacity decreases. This phenomenon may be explained by referring to OH^- ion diffusion processes during the charging/discharging for the electrode. When the electrode at high sweep rates corresponds to a high current density,

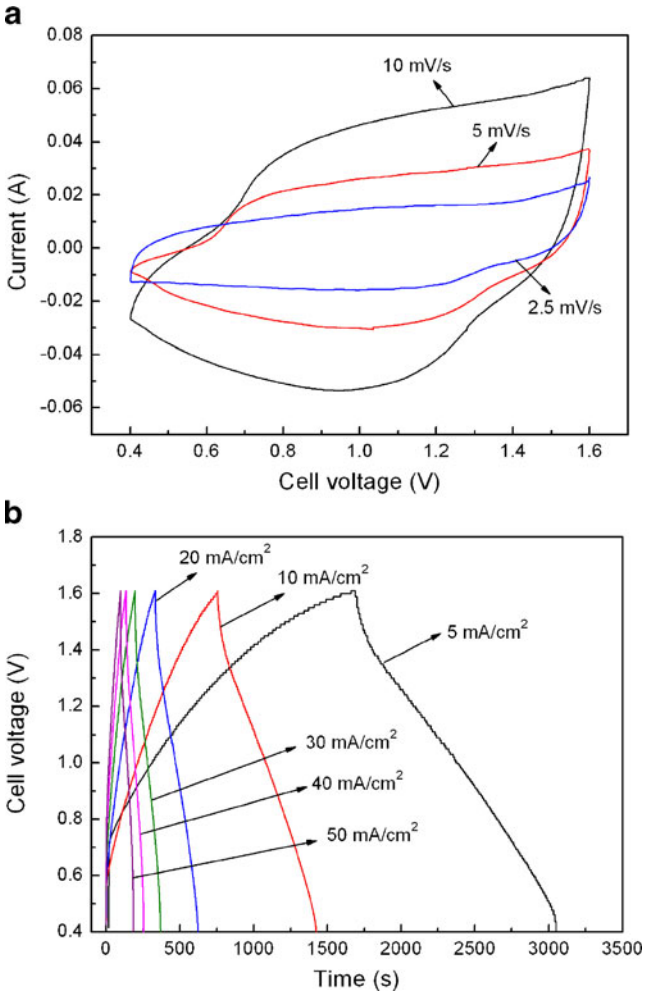

Fig. 4 Electrochemical properties of the asymmetric supercapacitor in 2 M KOH solution within a potential range from 0.4 to 1.6 V: **a** Cyclic voltammograms at different scan rates and **b** charge/discharge behavior at different current densities. The mass loads of the cathode 7.5% Al-substituted α-Ni(OH)$_2$ electrode material are 8 and 37.3 mg of the AC anode electrode material

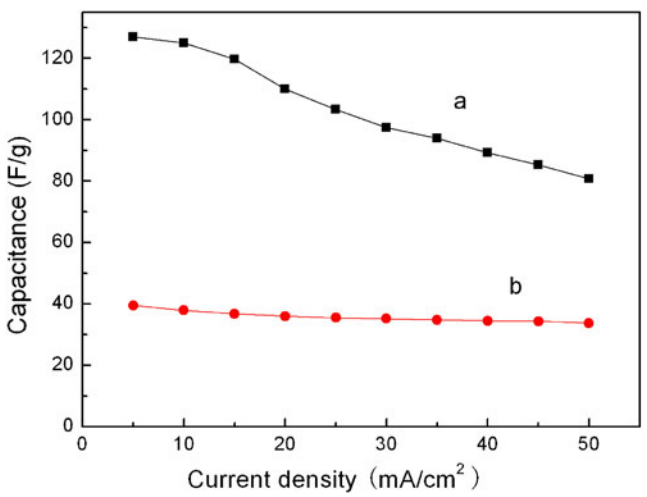

Fig. 5 Specific capacitance as a function of discharge currents for **a** asymmetric supercapacitor and **b** AC-based EDLC capacitor

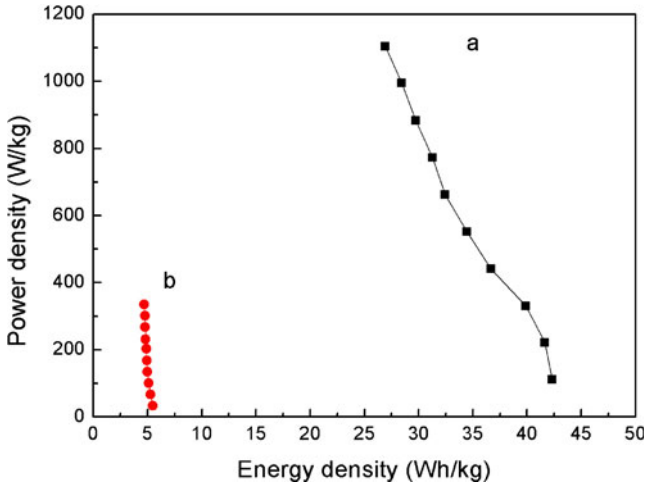

Fig. 6 Ragone plot relating power density to achievable energy density of **a** asymmetric supercapacitor and **b** AC-based EDLC capacitor

massive OH^- ions are required to intercalate swiftly at the interface of the electrode/electrolyte. However, relatively low concentration of OH^- ions could not meet this demand, and the processes would be controlled by the ion diffusion [34].

In comparison with the asymmetric capacitor, we fabricated a two-electrode AC symmetric capacitor and it was cycled galvanostatically between 0 and 1.0 V. Each electrode contained about 37.3 mg of AC material and had a geometric surface area of about 1 cm^2. Figure 5 shows the specific capacitance of the double electrode cell as a function of the discharge current density for the 7.5% Al-substituted α-Ni(OH)$_2$ electrode-based asymmetric supercapacitor and the AC-based EDLC. The specific capacitances of the hybrid capacitor of the total weight of the active material for both electrodes at 5, 10, 20, 30, 40, and 50 mA/cm^2 were 127, 125, 110, 97.4, 89.2, and 80.8 F/g, respectively. The specific capacitances of the EDLC of the total weight of the active

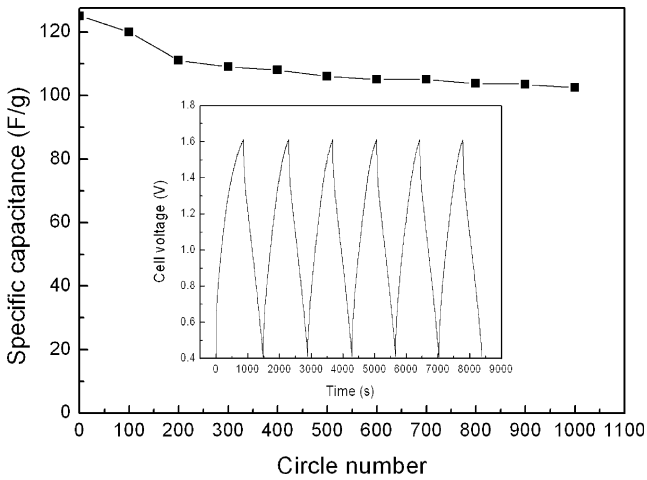

Fig. 7 Cycle life of the asymmetric supercapacitor at the current densities of 10 mA/cm^2. The inset is charge/discharge curves of the asymmetric supercapacitor

material for both electrodes at 5, 10, 20, 30, 40, and 50 mA/cm^2 were 39.5, 37.9, 36, 35.2, 34.5, and 33.7 F/g, respectively. The results show that the specific capacitance of the asymmetric supercapacitor is much higher than that of the EDLC. Even though under the large current density of 50 mA/cm^2, nearly 63.6% of the initial amount can be reached for the hybrid capacitor, so the large specific energy and good rate capability of the asymmetric capacitor make it attractive particularly for a practical application. This all demonstrates that the Al-substituted α-Ni(OH)$_2$ samples make it attractive particularly for a practical application of supercapacitor.

To highlight the electrochemical performance of the hybrid supercapacitor based on Al-substituted α-Ni(OH)$_2$ and AC electrodes, the Ragone plot relating real power density to energy density of the asymmetric supercapacitor and the EDLC is also demonstrated in Fig. 6. The energy and power data are calculated when taking account of only the mass of the electrode material. Clearly both the energy and power densities greatly increased compared with the EDLC type. This can be explained by the energy and power densities, which critically depend on the real working voltage. The energy density of the asymmetric supercapacitor increases from 26.9 to 42.3 W·h/kg, whereas the real power density from 1.10×10^3 to 110 W/kg. The specific energy increases by more than seven times compared with that of a symmetric AC-based EDLC capacitor using an aqueous KOH electrolyte.

The cycling stability of the asymmetric supercapacitor was performed by charge–discharge at a current density of 10 mA/cm^2 within a voltage range of 0.4–1.6 V in the 2 M KOH electrolyte. As shown in Fig. 7, the capacitance of the hybrid supercapacitor decreases with the growth of the cycle number. After continuous 1,000 cycles, the capacitance value remains 82% of that of the early cycle. The attenuation of the capacitance just for 18% suggests the good stability of the Ni(OH)$_2$/AC asymmetric supercapacitor, which is significant for the practical application.

Conclusion

In summary, Al-substituted α-Ni(OH)$_2$ materials were successfully prepared using a coprecipitation method. The experimental results of XRD show that the presence of dissolved cations such as Al in alkaline electrolyte can suppress the $\alpha\rightarrow\beta$-nickel hydroxide transformation. The specific capacitance of the 7.5% Al-substituted α-Ni(OH)$_2$ electrode at 5 mA/cm^2 is 2.08×10^3 F/g, which shows better rate capability and great potential as the electrode materials for electrochemical capacitors. An asymmetric supercapacitor based on 7.5% Al-substituted α-Ni(OH)$_2$ as the positive electrode and AC as the negative electrode with high operating voltage, high energy density, and maximum power density was fabricated in the 2 M KOH electrolyte. The specific capacitance and specific energy of the cell reached 127 F/g and 42.3 W·h/kg within the potential range from 0.4 to 1.6 V, respectively. The hybrid supercapacitor also demonstrated a good cycling performance with an attenuation of capacitance of 18% over 1,000 cycle numbers.

Acknowledgements This work was supported by the National Natural Science Foundation of China (no. 50602020) and the National Basic Research Program of China (no. 2007CB216408).

References

1. Toupin M, Brousse T, Bélanger D (2004) Chem Mater 16:3184
2. Conway BE (1991) J Electrochem Soc 138:1539
3. Winter M, Brodd RJ (2004) Chem Rev 104:4245
4. Park JH, Kim S, Park OO, Ko JM (2006) Appl Phys A 82:593
5. Brousse T, Taberna PL, Crosnier O, Dugas R, Guillemet P, Scudeller Y, Zhou Y, Favier F, Bélanger D, Simon P (2007) J Power Sources 173:633
6. Khomenko V, Raymundo-piñero E, Frackowiak E, Béguin F (2006) Appl Phys A 82:567
7. Yuan CZ, Gao B, Zhang XG (2007) J Power Sources 173:606
8. Yoon JH, Bang HJ, Prakash J, Sun YK (2008) Mater Chem Phys 110:222
9. Xue Y, Chen Y, Zhang ML, Yan YD (2008) Mater Lett 62:3884
10. An KH, Kim WS (2001) Adv Funct Mater 11:387
11. Wang DW, Li F, Liu M, Lu GQ, Cheng HM (2008) Angew Chem Int Ed 47:373
12. Cao L, Xu F, Liang YY, Li HL (2004) Adv Mater 16:1853
13. Ke YF, Tsai DS, Huang YS (2005) J Mater Chem 15:2122
14. Kong LB, Zhang J, An JJ, Luo YC, Kang L (2008) J Mater Sci 43:3664
15. Zhang J, Kong LB, Wang B, Luo YC, Kang L (2009) Synth Met 159:260
16. Huggins RA (2000) Solid State Ion 134:179
17. Zheng JP, Cygan PJ, Jow TR (1995) J Electrochem Soc 142:2699
18. Cottineau T, Toupin M, Delahaye T, Brousse T, Bélanger D (2006) Appl Phys A 82:599
19. Wang XF, You Z, Yuan DB (2006) Chin J Chem 24:1126
20. Palmas S, Ferrara F, Vacca A, Mascia M, Polcaro AM (2007) Electrochim Acta 53:400
21. Kong LB, Lang JW, Liu M, Luo YC, Kang L (2009) J Power Sources 194:1194
22. Srinivasan V, Weidner JW (1997) J Electrochem Soc 144:L210
23. Lang JW, Kong LB, Wu WJ, Luo YC, Kang L (2009) J Mater Sci 44:4466
24. Song QS, Li YY, Lchan SL (2005) J Appl Electrochem 35:157
25. Cheng J, Cao GP, Yang YS (2006) J Power Sources 159:734
26. Jayashree RS, Kamath PV (2001) J Appl Electrochem 31:1315
27. Yang GW, Xu CL, Li HL (2008) Chem Commun 48:6537
28. Kamath PV, Dixit M, Indira L, Shukla AK, Kumar VG, Munichandraiah N (1994) J Electrochem Soc 141:2956
29. Lang JW, Kong LB, Wu WJ, Liu M, Luo YC, Kang L (2009) J Solid State Electrochem 13:333
30. Lang JW, Kong LB, Wu WJ, Luo YC, Kang L (2008) Chem Commun 35:4213
31. Cao L, Lu M, Li HL (2005) J Electrochem Soc 152:A871
32. Wang XF, Ruan DB, You Z (2006) Trans Nonferrous Met Soc China 16:1129
33. Li YM, Li WY, Chou SL, Chen J (2008) J Alloys Compd 456:339
34. Kötz R, Carlen M (2000) Electrochim Acta 45:2483